Polymer, 1991, Vol. 32, 170–180

The umbrella shape of star polymers in the theta state*

Fabio Ganazzoli†, Mónica A. Fontelos and Giuseppe Allegra
Dipartimento di Chimica, Politecnico di Milano, Piazza L. da Vinci 32, I-20133 Milano, Italy
(Received 27 November 1989; revised 13 March 1990; accepted 26 March 1990)

The chain conformation in the theta state is calculated by self-consistent free-energy minimization assuming that the overall long-range two- and three-body interactions mutually compensate. However, the repulsive screened interactions arising from the intrinsic chain thickness do survive, imparting an asymptotically finite expansion to the chain. Because of the medium-range character of these interactions, the proportionality between the unperturbed mean-square radius of gyration $\langle S^2\rangle_0$ and the molecular weight is asymptotically maintained. Compared with the phantom chain, devoid of both intrinsic thickness (i.e. screened interactions) and long-range interactions, the arms experience an increasing expansion upon increasing the number of arms, f. At the same time, the fluctuations of the branch point around the centre of mass do increase as well, since the average angle between the arms *decreases*, and the macromolecule tends towards an umbrella-like shape. As a consequence, the macromolecular density becomes more uniform than for the phantom chain. This is reflected in the calculated structure factor $S(Q)$ by a sharpening of the peak in the plot of $Q^2S(Q)$ *versus* Q (where $Q = 4\pi \sin(\theta/2)/\lambda$), in good agreement with the experimental results by Huber *et al.* Through cancellation of contrasting effects, the topological index $g = \langle S^2\rangle_0/\langle S^2\rangle_{0,\text{linear}}$ is close to the value of the phantom chain for any f, whereas $h = R_{H0}/R_{H0,\text{linear}}$, R_H being the hydrodynamic radius, and $\rho = \langle S^2\rangle_0^{1/2}/R_{H0}$ are somewhat larger. The negligible influence of the residual three-body interactions in the theta state compared to the screened interactions is finally commented upon considering also recent Monte Carlo simulations.

(Keywords: theta state; star polymers; self-consistent approach; free-energy minimization; chain thickness)

INTRODUCTION

Star polymers are nowadays of great interest both because of their practical importance and as a check of current theories on polymer equilibrium and dynamics. Relatively monodisperse and well characterized samples have been synthesized in recent years[1–3], so that some experimental data are now available[1,2,4–9].

In the unperturbed Θ state the long-range two- and three-body interactions among chain atoms may be considered as absent, on average, because of mutual cancellation[10]. Using this criterion, we recently calculated[11] the Θ temperature of linear and regular star polymers as a function of the number of arms and of molecular weight. It turns out that Θ is smaller than expected for a polymer devoid of any long-range interaction because slightly attractive two-body attractions must counterbalance the repulsive three-body interactions, the more so the larger the number of arms or the smaller the molecular weight. Here we will address the question of the polymer conformation in the Θ state, assuming that only short-range and medium-range interactions are present[10].

The macromolecule will be described by an equivalent bead-and-spring model with Gaussian distributions of the interbead distances and will comprise $N+1$ beads and f arms of equal length, thus having N/f beads per arm, if one bead is at the branch point; in the following we shall be mainly concerned with the limit $N/f \to \infty$. In this description, short-range correlations among skeletal rotations are effectively neglected, being embodied in the segment of mean-square length l^2 connecting two adjacent beads. It should be stressed here that *the use of a Gaussian distribution does not imply a random-walk chain model*, in that the mean-square distance between two beads need not be proportional to their topological separation, in general. The equilibrium conformation is obtained by self-consistent minimization of the chain free energy[10], which is written as a sum of an elastic term and of a screened-interactions term[12]. The former has an entropic origin and arises from the loss of degrees of freedom caused by any deviation from the random-walk conformation, whereas the latter can be described as a repulsive term due to the finite thickness of the chain. In fact, although the effective potential $\varepsilon(\boldsymbol{r})$ between two beads at a distance $\boldsymbol{r}$, including both two- and three-body interactions, is usually represented by a delta function, it actually consists of the sum of a positive (hence repulsive) term due to the co-volume at short separation and of a negative (i.e. attractive) term influenced by the solvent at larger separations[10,12]. (An analogous model was also independently proposed by Martin[13].) The volume integral of $\varepsilon(\boldsymbol{r})$ vanishes in the Θ state, meaning that the long-range repulsions are effectively compensated by the solvent-induced attractions. However, the mismatch between the regions of space where $\varepsilon(\boldsymbol{r})$ is repulsive and where it is attractive gives an overall free-energy repulsive term, not fully compensated by the screening effect of the solvent, proportional to

* Dedicated to Professor Walther Burchard on the occasion of his 60th birthday

† To whom correspondence should be addressed

0032-3861/91/010170-11

$\langle r^2(i,j)\rangle^{-5/2}$, where $\langle r^2(i,j)\rangle$ is the mean-square distance between beads i and j[12]. This repulsion is not of a long-range character, because it falls off fast enough with increasing $|i-j|$ that the proportionality between the mean-square radius of gyration and molecular weight is preserved. It may be regarded as a medium-range interaction[10] in that it has a much longer range than the correlation among the skeletal rotations, but not long enough to influence the above-mentioned proportionality.

In this paper we apply these concepts to star polymers, where these effects are enhanced by the density of segments at the branch point and where we may expect a delicate interplay between the repulsions *within* one arm and *among* the arms. The main emphasis will be on the calculation of the intramolecular mean-square distances, of the mean-square radius of gyration and, more briefly, of the hydrodynamic radius. The latter quantities are experimentally accessible, but they only reflect the overall behaviour of the polymer. A quantity more sensitive to the distribution of the intramolecular distances is the structure factor, measured through elastic neutron scattering to probe the local conformations; a section is therefore devoted to its calculation.

THE MATHEMATICAL APPROACH

The basic equations

As sketched in the 'Introduction', the free-energy terms due to long-range two- and three-body interactions cancel each other in the Θ state[10–12], apart from an irrelevant constant, so that the excess free energy over the random-walk phantom chain is, in k_BT units:

$$\mathscr{A} = (A - A_{ph})/k_BT = \mathscr{A}_{el} + \mathscr{A}_{2s} \qquad (1)$$

where A and A_{ph} are the actual and the phantom-chain free energy. In this context, we denote as phantom chain an infinitely thin chain where the skeletal atoms are completely insensitive to one another except for local correlation among skeletal rotations (these involve at most 5–10 bonds and are effectively included in the average segment length between adjoining beads). The reference phantom chain, indicated by a 'ph' subscript, is therefore devoid of any long-range or medium-range interaction. In the following, we will also use a zero subscript for the average quantities of the unperturbed polymer and no subscript at all for relationships of more general validity. In equation (1), $\mathscr{A}_{el}$ is the elastic contribution and $\mathscr{A}_{2s}$ is the (repulsive) medium-range contribution due to the two-body screened interactions[10,12] originating from the intrinsic chain thickness. Within the Gaussian approximation, we have[12]:

$$\mathscr{A}_{2s} = (K_0/2)\sum_{i\neq j}\sum \langle r^2(i,j)\rangle^{-5/2} \qquad |i-j| \geq \bar{k} \quad (2)$$

where

$$K_0 = \frac{3}{2}(3/2\pi)^{3/2} v_c \langle \Delta^2 r\rangle \qquad (2a)$$

is the parameter of the screened interactions. Here, $\langle \Delta^2 r\rangle$ is the mean-square chain thickness, v_c is the co-volume per chain bead and $\bar{k}$ is a lower cut-off originating from stereochemical constraints that prohibits any two atoms separated by $k < \bar{k}$ bonds to come into contact. $\bar{k}$ turns out to be somewhat larger than the statistical segment length; accordingly, in the present context, it will have the value of a few segment units.

The elastic free energy is best expressed as a sum over the chain normal modes[10,14] to account for all the degrees of freedom. The normal modes of a phantom-chain star polymer were first obtained by Zimm and Kilb[15] and may be expressed as a trigonometric Fourier transform of the bond vectors. Owing to the star symmetry, these modes are formally equal, though with a different multiplicity, to those of the linear chain formed by two arms only of the star, therefore having $m = 2N/f + 1$ beads. Let us label sequentially the beads of this linear chain from 1 to $2N/f + 1$, so that the branch point is labelled as $N/f + 1$ and the free ends as 1 and $2N/f + 1$; the normal modes are[10]:

$$\tilde{\boldsymbol{l}}(q) = 2^{1/2}\sum_{i=1}^{2N/f} \boldsymbol{l}(i)\,\sin[q(i-1)] \qquad (3)$$

where $\boldsymbol{l}(i)$ is the ith bond vector connecting beads i and $i+1$ ($i = 1, 2, \ldots, 2N/f$) and q is the Fourier coordinate:

$$q = (\pi/m)n_q \qquad n_q = 1, 2, \ldots, m-1 \ (m = 2N/f + 1) \qquad (4)$$

The corresponding inverse transform is:

$$\boldsymbol{l}(i) = (2^{1/2}/N)\sum_{\{q\}} \tilde{\boldsymbol{l}}(q)\,\sin[q(i-1)] \qquad (5)$$

In other words, we need only consider two arms, the others being taken care of by symmetry through the multiplicity of the modes[15]: the even modes, i.e. those with n_q even, have a unit multiplicity, whereas the odd modes (with n_q odd) have a multiplicity $f-1$. With the above labelling scheme the symmetry properties of the transform are somewhat hidden, but many expressions are more concise and computationally simpler. We shall assume as a first approximation that the normal modes $\tilde{\boldsymbol{l}}(q)$ remain orthogonal (i.e. $\langle \tilde{\boldsymbol{l}}(q)\cdot\tilde{\boldsymbol{l}}(q')\rangle = 0$ if $q \neq q'$) even in the presence of the Θ expansion due to the screened interactions. Accordingly, the mean-square distance between beads i and j can be written as a single sum over the normal modes:

$$\langle r^2(i,j)\rangle = \frac{2l^2}{m}\sum_{\{q\}} \tilde{\alpha}^2(q) \times \frac{\sin^2[q(i-j)/2]\,\sin^2[q(i+j-1)/2]}{\sin^2(q/2)} \qquad (6)$$

where $\tilde{\alpha}^2(q)$ is the expansion factor of the mean-square amplitude of the q mode:

$$\tilde{\alpha}^2(q) = \langle|\tilde{\boldsymbol{l}}^2(q)|^2\rangle / \langle|\tilde{\boldsymbol{l}}^2(q)|^2\rangle_{ph} \qquad (6a)$$

It may be shown that in the above sum the even modes give a larger contribution when i and j belong to the same arm and the odd modes when i and j are on different arms.

Note that for $\tilde{\alpha}^2(q) \equiv 1$ we recover the random-walk phantom-chain result:

$$\langle r^2(i,j)\rangle_{ph} = l^2|i-j| \qquad (7)$$

In other words, in the phantom chain the mean-square distance between any two beads depends only on their topological separation, and not on their location within the chain, whereas this is not so in general.

The elastic free energy $\mathscr{A}_{el}$ can now be expressed as:

$$\mathscr{A}_{el} = \frac{3}{2}\sum_{\{q\}} \varphi[\tilde{\alpha}^2(q) - 1 - \ln\tilde{\alpha}^2(q)] \qquad (8)$$

where

$$\varphi = \begin{cases} 1 & \text{for even modes} \\ f-1 & \text{for odd modes} \end{cases} \tag{8a}$$

The unperturbed chain conformation is obtained by minimization of the excess free energy $\mathscr{A}$ with respect to all the degrees of freedom. Using equations (8) and (2) together with equation (6), from the condition $\partial\mathscr{A}/\partial\tilde{\alpha}^2(q) = 0$ we get:

$$\frac{1}{\tilde{\alpha}^2(q)} = 1 - \frac{5}{3}\frac{K}{\varphi m}\frac{1}{\sin^2(q/2)}\sum_{i\neq j}\sum \sin^2[q(i-j)/2] \times \sin^2[q(i+j-1)/2]/J(i,j)^{7/2} \tag{9}$$

($|i-j| \geqslant \bar{k}$, $m = 2N/f + 1$) where K is the dimensionless parameter of the screened interactions:

$$K = K_0/l^5 \tag{9a}$$

and we define:

$$J(i,j) = \langle r^2(i,j)\rangle_0/l^2 \tag{9b}$$

(Note that in equation (9) the linear chain is given by $f = 2$ only, while $f = 1$ must be excluded.)

Equations (6) and (9) form a set of coupled equations, which must be solved self-consistently. From inspection of equation (9), it may be seen that for $f > 2$ the expansion factor of the even modes is larger than that of the odd modes, the ratio $[1 - 1/\tilde{\alpha}^2(q)]_{\text{even}}/[1 - 1/\tilde{\alpha}^2(q)]_{\text{odd}}$ tending approximately to $(f-1)$ for $q \ll 1$.

Note that, owing to the star symmetry, the double sum in equation (9) can be split into two smaller double sums as follows:

$$\sum_{i\neq j}\sum \rightarrow f\sum_{i=1}^{N/f}\left(2\sum_{j=i+1}^{N/f+1} + (f-1)\sum_{j=N/f+2}^{2(N/f+1)-i} w_{ij}\right) \tag{10}$$

$$w_{ij} = \begin{cases} 1 & \text{if } i+j = 2(N/f+1) \\ 2 & \text{otherwise} \end{cases}$$

with greater computational efficiency.

From a self-consistent set $\{\tilde{\alpha}^2(q)\}$ and $\{\langle r^2(i,j)\rangle_0\}$, we may calculate other quantities of interest, like the mean-square radius of gyration $\langle S^2\rangle_0$, the hydrodynamic radius R_{H0} and the structure factor $S(Q)$ (Q is the modulus of the scattering vector: $Q = 4\pi\sin(\theta/2)/\lambda$, λ being the wavelength employed and θ the scattering angle):

$$\langle S^2\rangle = \frac{1}{2(N+1)^2}\sum_{i,j}\sum\langle r^2(i,j)\rangle = \frac{fl^2}{m(N+1)^2}\sum_{\{q\}}\frac{\tilde{\alpha}^2(q)}{4\sin^2(q/2)}[A(q) + (f-1)B(q)] \tag{11}$$

where

$$A(q) = \left(\frac{N}{f}+1\right)^2 + \frac{(-1)^{n_q}}{2}\left(\frac{N}{f}+1\right) - \frac{1-(-1)^{n_q}\cos q}{4\sin^2(q/2)}$$

$$B(q) = \left(\frac{N}{f}\right)^2 - \frac{(-1)^{n_q}}{2}\frac{N}{f} - (-1)^{n_q}\frac{1-(-1)^{n_q}\cos q}{4\sin^2(q/2)} \tag{11a}$$

$$R_H = (N+1)^2\left(\sum_{i\neq j}\sum\langle r^{-1}(i,j)\rangle\right)^{-1} = (N+1)^2(\pi/6)^{1/2}\left(\sum_{i\neq j}\sum\langle r^2(i,j)\rangle^{-1/2}\right)^{-1} \tag{12}$$

$$S(Q) = (N+1)^{-2}\sum_{h,j}\sum\langle\exp[-i\boldsymbol{Q}\cdot\boldsymbol{r}(h,j)]\rangle = (N+1)^{-2}\sum_{h,j}\sum\exp\left(-\frac{Q^2}{6}\langle r^2(h,j)\rangle\right) \tag{13}$$

within the Gaussian approximation.

$\langle S^2\rangle$ is defined as the mean-square distance of the polymer beads from the centre of mass, but, as pointed out long ago by Zimm and Stockmayer[16], it is usefully expressed as the difference between the mean-square distances of the beads from a reference bead, $\langle X^2\rangle$, and the mean-square distance of the latter from the centre of mass, $\langle Z^2\rangle$. In a star polymer the most natural reference bead is the branch point, so that:

$$\langle S^2\rangle = \langle X^2\rangle - \langle Z^2\rangle \tag{14}$$

$$\langle X^2\rangle = \frac{1}{N+1}\sum_{i=1}^{N+1}\langle r^2(i,N/f+1)\rangle = \frac{f}{N+1}\sum_{i=1}^{N/f}\langle r^2(i,N/f+1)\rangle \tag{14a}$$

$$\langle Z^2\rangle = \frac{1}{2(N+1)^2}\sum_{i,j}\sum[\langle r^2(i,N/f+1)\rangle + \langle r^2(j,N/f+1)\rangle - \langle r^2(i,j)\rangle] \tag{14b}$$

$\langle X^2\rangle$ may also be given as a sum over the normal modes:

$$\langle X^2\rangle = \frac{fl^2}{N+1}\sum_{\{q\}}\frac{\tilde{\alpha}^2(q)}{4\sin^2(q/2)}\left(1 + \frac{(-1)^{n_q}}{2}\right) \tag{15}$$

whereas the corresponding expression for $\langle Z^2\rangle$ is rather cumbersome; therefore, this quantity is most easily evaluated from $\langle S^2\rangle$ and $\langle X^2\rangle$ through equation (14).

A first-order perturbative approach: analytical results

The Θ expansion of a star polymer may be evaluated analytically from equations (6) and (9) assuming the screened interactions to be a small perturbation over the phantom chain, thus implying that the effective parameter Kf will be small compared to unity. We will consider a star polymer with very long arms, that is with $N/f \gg 1$, so that the collective modes of interest have $q \ll 1$. Let us start with the phantom chain, for which $\tilde{\alpha}^2(q) \equiv 1$, therefore $\langle r^2(i,j)\rangle_{\text{ph}} = l^2|i-j|$ (see equation (7)). Replacing now this expression in equation (9) and taking into account equation (10), we can get the leading term of $\tilde{\alpha}^2(q)$ (see the Appendix, equation (A.2))[12]:

$$\frac{1}{\tilde{\alpha}^2(q)} \simeq \frac{1}{\tilde{\alpha}^2(0)} + \frac{5}{3}K\frac{f}{\varphi}Gq^{1/2} \tag{16}$$

where (see equation (A.3))

$$\frac{1}{\tilde{\alpha}^2(0)} \equiv \frac{1}{\tilde{\alpha}^2(q)}\Big|_{q\rightarrow 0} = 1 - \frac{5}{3}\frac{K}{(\bar{k})^{1/2}}\frac{f}{\varphi} + O\left[\left(\frac{N}{f}\right)^{-1/2}\right] \tag{16a}$$

(Here, it is understood that q tends to zero separately for even or odd modes.) We point out that these terms arise from the interaction between relatively close beads having $|i-j| \simeq \bar{k}$ (see equation (A.3)), in keeping with the medium-range character of the potential. In equation (16) the constant G is defined through:

$$G = 2^{-3/2}\int_0^\infty \frac{x^2 - \sin^2 x}{x^{7/2}}\,dx = 0.6684 \tag{17}$$

The upper limit of this integral was set to infinity for

simplicity (see equation (A.4) and the following discussion): this implies that equation (16) is slightly approximate for the first two or three even and odd modes, which may entail some inaccuracy in the derived quantities for small arm lengths. On the other hand, the q-dependent term in equation (16) becomes negligible anyway when considering the collective modes of very long chains, so that we may put, from equations (16) $(K/(\bar{k})^{1/2} \ll 1)$:

$$\tilde{\alpha}^2(q)|_{q\to 0} = \begin{cases} 1 + \dfrac{5}{3}\dfrac{K}{(\bar{k})^{1/2}} f = \tilde{\alpha}^2_{\text{even}} & \text{(even modes)} \\ 1 + \dfrac{5}{3}\dfrac{K}{(\bar{k})^{1/2}} \dfrac{f}{f-1} = \tilde{\alpha}^2_{\text{odd}} & \text{(odd modes)} \end{cases} \tag{18}$$

neglecting terms of the order of $(N/f)^{-1/2}$ (see equations (A.3)).

This expression can be inserted in equation (6) to obtain the mean-square distances upon performing separately the sums with n_q even or odd (setting the upper limits to infinity since the largest contribution is due to the collective modes with $q \ll 1$). For symmetry reasons, we need only calculate the distances between one bead in a given arm, that is, with $1 \leqslant i < N/f + 1$, and the second bead either within the same arm (that is, with $i < j \leqslant N/f + 1$) or in another arm with $N/f + 1 \leqslant j \leqslant 2(N/f + 1) - i$:

$$\langle r^2(i,j)_0\rangle_0 = l^2(j-i)\sigma_1 \qquad 1 \leqslant i < j \leqslant N/f + 1 \tag{19a}$$

$$\langle r^2(i,j)\rangle_0 = l^2(j-i)\sigma_1 - 2l^2[j - (N/f+1)]\sigma_2 \qquad N/f + 1 \leqslant j \leqslant 2(N/f+1) - i \tag{19b}$$

where

$$\sigma_1 = (\tilde{\alpha}^2_{\text{even}} + \tilde{\alpha}^2_{\text{odd}})/2 \simeq 1 + \frac{5}{6}\frac{K}{(\bar{k})^{1/2}}\frac{f^2}{f-1}$$
$$\sigma_2 = (\tilde{\alpha}^2_{\text{even}} - \tilde{\alpha}^2_{\text{odd}})/2 \simeq \frac{5}{6}\frac{K}{(\bar{k})^{1/2}}\frac{f(f-2)}{f-1} \tag{19c}$$

The phantom chain is recovered by setting $K/(\bar{k})^{1/2} = 0$, thus putting $\sigma_1 \equiv 1$ and $\sigma_2 \equiv 0$. Also, for the linear chain ($f = 2$) $\tilde{\alpha}^2_{\text{even}} = \tilde{\alpha}^2_{\text{odd}}$, so that $\sigma_2 \equiv 0$ and the two regimes of $\langle r^2(i,j)\rangle_0$ reduce to one (this would also be true for a perturbed chain).

In the same way, we may also get the corresponding first-order expressions for $\langle S^2\rangle_0$, $\langle X^2\rangle_0$ and $\langle Z^2\rangle_0$ using equations (18) or (19) with equations (11), (14) and (15):

$$\langle S^2\rangle_0 = \frac{l^2}{6}\frac{N}{f}\left(\sigma_1\frac{3f-2}{f} - 2\sigma_2\frac{f-1}{f}\right) \simeq \frac{l^2}{6}\frac{N}{f}\left(\frac{3f-2}{f} + \frac{5}{6}\frac{K}{(\bar{k})^{1/2}}\frac{f^2+4(f-1)}{f-1}\right) \tag{20}$$

$$\langle X^2\rangle_0 = \frac{l^2}{2}\frac{N}{f}\sigma_1 \simeq \frac{l^2}{2}\frac{N}{f}\left(1 + \frac{5}{6}\frac{K}{(\bar{k})^{1/2}}\frac{f^2}{f-1}\right) \tag{21}$$

$$\langle Z^2\rangle_0 = \frac{l^2}{3}\frac{N}{f}\left(\frac{\sigma_1}{f} + \sigma_2\frac{f-1}{f}\right) \simeq \frac{l^2}{3}\frac{N}{f}\left(\frac{1}{f} + \frac{5}{6}\frac{K}{(\bar{k})^{1/2}}\frac{f^2-2(f-1)}{f-1}\right) \tag{22}$$

From the above, we have $\langle S^2\rangle_0 \propto N$, thus confirming that we are indeed in the Θ state.

The perturbative expression for the hydrodynamic radius R_{H0} may be obtained from equations (12) and (19) treating the bead indices as continuous variables, thereby transforming the sums into integrals. The result is:

$$R_{\text{H0}}^{-1} = \frac{8}{3l}\left(\frac{6}{\pi}\right)^{1/2}\left(\frac{N}{f}\right)^{-1/2} \times \frac{1}{f}\left(\sigma_1^{-1/2} + (f-1)\frac{2^{1/2}(\sigma_1-\sigma_2)^{1/2} - \sigma_1^{1/2}}{\sigma_1 - 2\sigma_2}\right) \tag{23}$$

σ_1 and σ_2 being given in equation (19c).

The full self-consistent solution: numerical results

The set of coupled equations (6) and (9) was also solved numerically through an iterative procedure, as previously done by us[12,14], taking into account equation (10). Starting again from $\tilde{\alpha}^2(q) \equiv 1$, therefore from $\langle r^2(i,j)\rangle_{\text{ph}} = l^2|i-j|$ (see equation (7)), equations (9) and (10) yield an improved set $\{\tilde{\alpha}^2(q)\}$, which upon insertion in equation (6) gives a new set of $\langle r^2(i,j)\rangle_0$. The latter is recycled into equation (9) and so on until self-consistency is reached; of course, we checked that in so doing the excess free energy $\mathscr{A}$ was indeed minimized. A fixed value of the screened-interactions parameter $K/(\bar{k})^{1/2} = 0.09$ was used throughout, corresponding to that estimated by one of us[12] for atactic polystyrene; we also set the cut-off value $\bar{k}$ to 1 for simplicity. Since only two arms need be considered in the calculations, while the others are accounted for through multiplicity factors, we carried out the calculations for fixed arm lengths N/f increasing f stepwise from the initial value of 2 (linear chain) and using the self-consistent values of $\tilde{\alpha}^2(q)$ obtained for a given f as the starting point for a larger f to speed up convergence. Owing to computer time limitations, the largest N/f considered was 500.

The numerical results confirmed the first-order analytical results: a plot of $\tilde{\alpha}^2(q)$ *versus* $q^{1/2}$ (cf. equation (16)) is indeed linear at small q with a negative slope for both even and odd modes, so that we may write:

$$\tilde{\alpha}^2(q) = a - bq^{1/2} \qquad (q \ll 1) \tag{24}$$

a being either $\tilde{\alpha}^2_{\text{even}}$ or $\tilde{\alpha}^2_{\text{odd}}$ (see equation (18)) and b (>0) either b_{even} or b_{odd}. The $\tilde{\alpha}^2(q)$ values of the even modes are larger than those of the odd modes for any f (>2) and each set falls on a single curve independent of N/f with only minor deviations for the very first few modes. From the numerical results, $\tilde{\alpha}^2_{\text{even}}$ and $\tilde{\alpha}^2_{\text{odd}}$ are therefore obtained as a function of f by extrapolation to $q \to 0$. These values and the slopes b agree with the perturbative results (equations (16) and (18)) when plotted as a function of f, as shown in *Figure 1*. The numerical results deviate slightly from the perturbative ones at large f since the latter are valid to first order in $Kf/(\bar{k})^{1/2}$, while second-order terms become relevant for highly branched chains if $K/(\bar{k})^{1/2} = 0.09$.

At convergence, the mean-square distances $\langle r^2(i,j)\rangle_0$ follow the peculiar two-regime behaviour depending on whether i and j belong to the same or to different arms; typical plots of $\langle r^2(i,j)\rangle_0$ as a function of $j - i$ (for fixed i, $j > i$) are shown in *Figure 2* for $f = 6$ and $f = 12$ in suitably normalized variables together with the perturbative results of equations (19). (The normalized variables

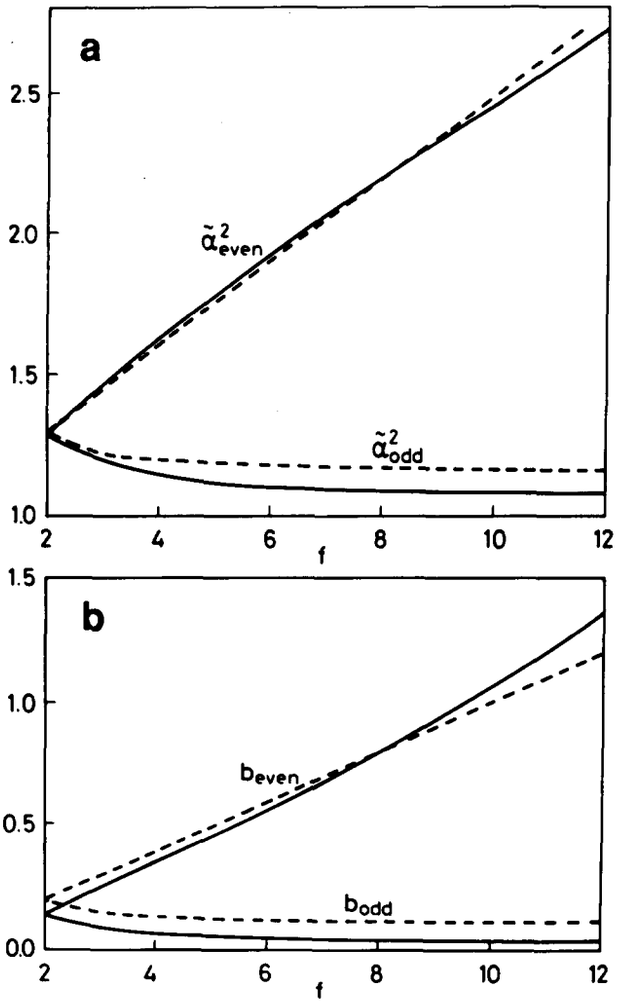

Figure 1 The intercepts $\tilde{\alpha}^2_{even}$, $\tilde{\alpha}^2_{odd}$ (a) and the slopes, with change of sign, b_{even}, b_{odd} (b) of $\tilde{\alpha}^2(q)$ *versus* $q^{1/2}$ (see equation (24)) plotted as a function of f. Full curves: numerical results ($N/f \to \infty$) with $K/\langle k \rangle^{1/2} = 0.09$, $k = 1$ (used throughout). Broken curves: the perturbative results with the same value of $K/\langle k \rangle^{1/2}$ as above (from equations (16) and (18)). (Although only integer values of f should be permitted, here and in the following we use an interpolating line for clarity)

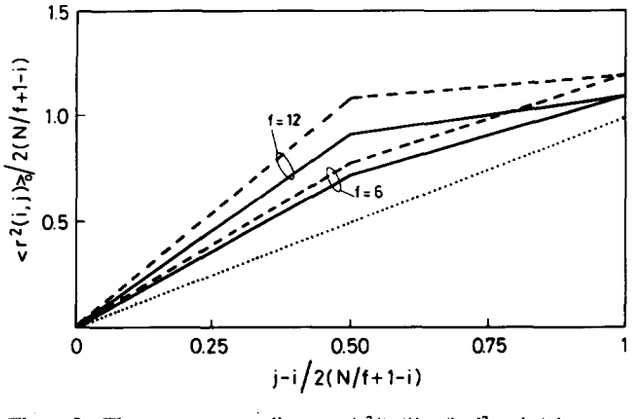

Figure 2 The mean-square distance $\langle r^2(i, j)\rangle_0$ (in l^2 units) between beads i and j as a function of their topological separation $j - i$ for fixed i ($j > i$), in normalized variables. Full lines: numerical results from full self-consistent approach. Broken lines: perturbative results from equations (19). Dotted line: the phantom-chain result. The variable on the abscissa was chosen so that the plot is valid for any i; it is 0 when j coincides with i, 0.5 when j is at the branch point (labelled $N/f + 1$) and 1 when j is in the position symmetrically opposite to i with respect to the branch point (i is always chosen in the first arm, so that $1 \leqslant i < N/f + 1$)

were chosen so that the plot is valid for *any* given value of i.) As a general trend, the slope *increases* with f when the beads belong to the same arm (value on the abscissa smaller than 0.5), whereas it *decreases* with f when the beads belong to different arms (value on the abscissa larger than 0.5).

A COMPARISON BETWEEN THE Θ-STATE EXPANSION OF LINEAR AND BRANCHED POLYMERS

As a result of the repulsive medium-range screened interactions due to the intrinsic chain thickness, a real polymer is somewhat expanded with respect to the random-walk phantom-chain model, although the proportionality between the mean-square radius of gyration $\langle S^2 \rangle_0$ and the molecular weight is asymptotically preserved (see equation (20)). Furthermore, with increasing number of arms f, a greater density of segments is present near the star core, hence a larger number of repulsive interactions between beads at short topological separation. These interactions force the arms to stretch outwards, thereby increasing the polymer size with respect to the phantom chain, the more so the larger is f, as shown by $\tilde{\alpha}^2_{even}$ (e.g. *Figure 1*). On the other hand, the very topology of a star polymer makes it a more compact object than a linear chain with the same total molecular weight. The degree of compactness is usually given in terms of topological indices, defined as:

$$g = \langle S^2 \rangle_0 / \langle S^2 \rangle_{0,\text{linear}} \tag{25a}$$

$$h = R_{H0} / R_{H0,\text{linear}} \tag{25b}$$

For the phantom-chain polymer we have[16,17]:

$$g_{ph} = (3f - 2)/f^2 \tag{26a}$$

$$h_{ph} = f^{1/2}/[1 + (f - 1)(2^{1/2} - 1)] \tag{26b}$$

Actually, these expressions hold only in the limit $N/f \gg 1$; this limit is reached quite soon by g_{ph}, unlike R_H, which depends on reciprocal averages, so that h_{ph} may be quite different from the limiting value even for relatively large molecular weights.

In *Figure 3* we show our asymptotic results for g and h; they show a close similarity with the phantom-chain values, particularly concerning g. However, at small f our curve is the lower one, thus suggesting an even greater compactness of the polymer than predicted for the phantom chain. This is at variance with h, which is always somewhat larger than h_{ph}, and, most important, in apparent contradiction with the qualitative expectation discussed above. The contradiction is even more apparent if we consider that g may be expressed as:

$$g = g_{ph}(\alpha_S^2/\alpha^2_{S,\text{linear}}) \tag{27}$$

where

$$\alpha_S^2 = \langle S^2 \rangle_0 / \langle S^2 \rangle_{ph} \tag{28}$$

is the expansion factor of the mean-square radius of gyration. A plot of the asymptotic values of α_S^2 *versus* f for large molecular weight is reported in *Figure 4* and shows a minimum for $f = 3$–4; note that the analogous plot of $\alpha_H = R_{H0}/R_{H,ph}$ reported in the same figure does not show any such minimum.

The anomaly in this behaviour can be explained by expressing $\langle S^2 \rangle_0$ through the difference between the mean-square distance of the beads from the branch point,

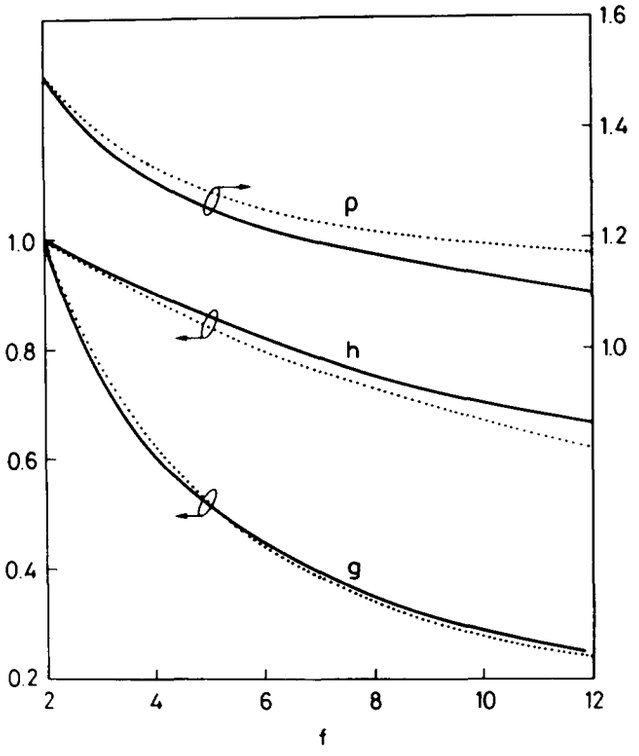

Figure 3 The topological ratios $g = \langle S^2\rangle_0/\langle S^2\rangle_{0,\text{linear}}$, $h = R_{H0}/R_{H0,\text{linear}}$ and $\rho = \langle S^2\rangle_0^{1/2}/R_{H0}$ plotted as a function of f. Full curves: numerical results. Dotted curves: phantom-chain results[16,17]. The perturbative results are not shown for clarity, being essentially coincident with the numerical ones

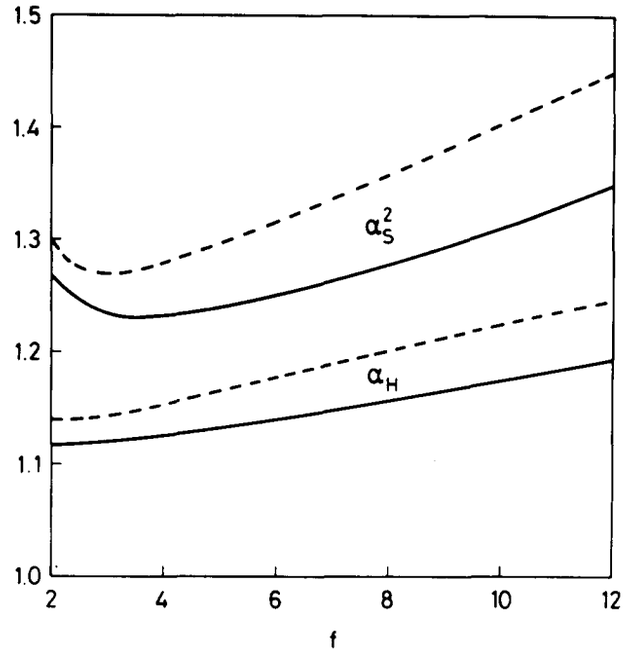

Figure 4 The expansion factors $\alpha_S^2 = \langle S^2\rangle_0/\langle S^2\rangle_{ph}$ and $\alpha_H = R_{H0}/R_{H,ph}$ as a function of f. Full curves: numerical results. Broken curves: perturbative results

$\langle X^2\rangle_0$, and the mean-square distance of the latter from the centre of mass, $\langle Z^2\rangle_0$ (see equations (14)). Let us first consider the phantom-chain polymer (see equations (21) and (22) with $K/(\bar{k})^{1/2} \equiv 0$). Upon joining an increasing number of arms of given length N/f to a common point, $\langle X^2\rangle_{ph}$ is independent of f, whereas $\langle Z^2\rangle_{ph}$ decreases proportionally to $1/f$. In other words, the arms do not interact and can intersect freely, so that $\langle X^2\rangle_{ph}$ is a constant for a fixed arm length. However, the increase in f displaces the centre of mass towards the branch point and therefore decreases $\langle Z^2\rangle_{ph}$ so that in the limit $f \to \infty$ the centre of mass and the branch point coincide (i.e. $\langle Z^2\rangle_{ph} \to 0$). Correspondingly, $\langle S^2\rangle_{ph}$ increases with f at fixed N/f to a finite value, with $\langle S^2\rangle_{ph} \simeq \langle X^2\rangle_{ph}$ for $f \to \infty$.

Conversely, in the presence of the screened interactions $\langle X^2\rangle_0$ increases monotonically with f for a fixed arm length N/f due to the larger number of repulsions between topologically neighbouring beads close to the star core: the ratio $\alpha_X^2 = \langle X^2\rangle_0/\langle X^2\rangle_{ph}$ is reported in *Figure 5* together with the perturbative result from equation (21). $\langle Z^2\rangle_0$ follows a more complex pattern since it depends on two contrasting effects (see also equation (22)): for fixed N/f, the centre of mass would approach the branch point upon increasing f, as in the phantom-chain model; but at the same time the two points are taken farther apart by the increased interbead repulsions. For lightly branched chains (small f), the first contribution is more important and $\langle Z^2\rangle_0$ decreases somewhat with f, whereas the opposite is true at larger f. However, $\langle Z^2\rangle_0$ is always larger than $\langle Z^2\rangle_{ph}$ and $\alpha_Z^2 = \langle Z^2\rangle_0/\langle Z^2\rangle_{ph}$ increases monotonically with f much more quickly than α_X^2, becoming very large at large f as shown in *Figure 5*. The increase of $\langle Z^2\rangle_0$ over the phantom-chain value (see equation (14b)) is essentially due to the faster increase of $\langle r^2(i,j)\rangle_0$ with $|i-j|$ for beads belonging to the *same* arm compared to beads belonging to *different* arms, the more so the larger is f (see *Figure 2*). This finding suggests an interesting consideration concerning the space correlation between the average directions of the arms. Let us consider (see

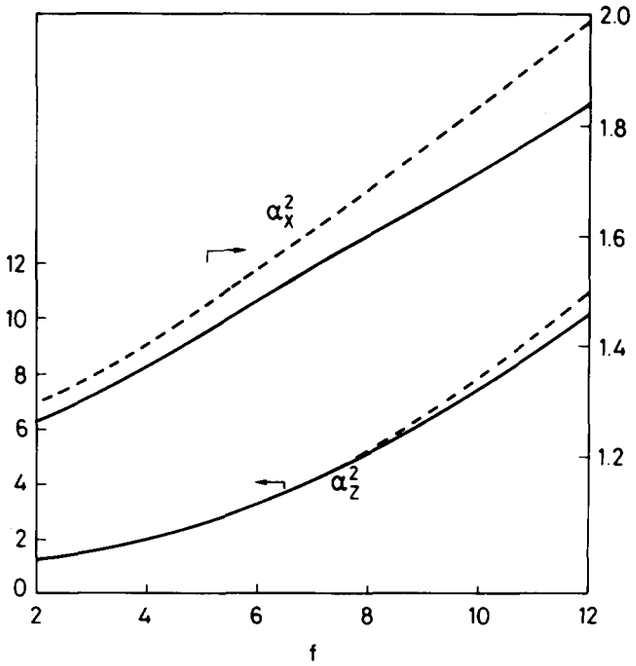

Figure 5 The expansion factors of the mean-square distance of the chain beads from the branch point, $\alpha_X^2 = \langle X^2\rangle_0/\langle X^2\rangle_{ph}$, and of the mean-square distance of the branch point from the centre of mass, $\alpha_Z^2 = \langle Z^2\rangle_0/\langle Z^2\rangle_{ph}$, *versus* the number of arms f. Full curves: numerical results. Broken curves: perturbative results

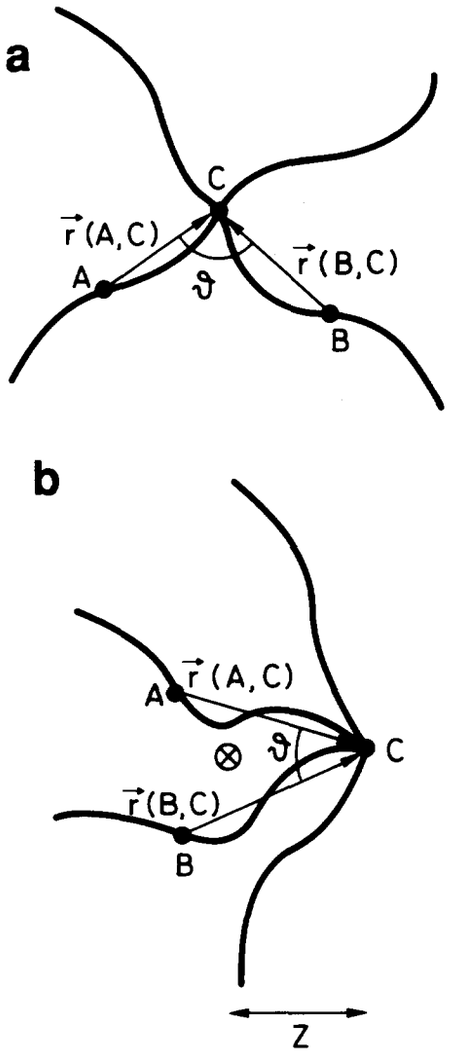

Figure 6 (a) Definition of the angle θ between vectors r(A, C) and r(B, C) placed on different arms. (b) A large value of $\langle Z^2\rangle_0$ means a large displacement Z of the centre of mass ⊗ from the branch point C, which in turn is related to inter-arm angles θ averaging less than 90° (see text). With this closing up of the arms, the star polymer tends to assume an umbrella-like shape

Figure 6) two beads, A and B, placed on different arms at the same topological distance from the branch point C (using the numbering scheme adopted before, A corresponds to bead i, B to bead $2(N/f+1)-i$ and C to bead $N/f+1$). The angle θ between r(A, C) and r(B, C) is given by:

$$r^2(\mathrm{A},\mathrm{B}) = r^2(\mathrm{A},\mathrm{C}) + r^2(\mathrm{B},\mathrm{C}) - 2|r(\mathrm{A},\mathrm{C})|\,|r(\mathrm{B},\mathrm{C})|\cos\theta \tag{29}$$

Let us assume to a first approximation that $|r(\mathrm{A},\mathrm{C})|$, $|r(\mathrm{B},\mathrm{C})|$ and θ are statistically uncorrelated, and take the average of equation (29). Since $\langle|r|\rangle = (8\langle r^2\rangle/3\pi)^{1/2}$ if r is a Gaussian-distributed vector, and $\langle r^2(\mathrm{A},\mathrm{C})\rangle_0 = \langle r^2(\mathrm{B},\mathrm{C})\rangle_0$, we have (see also equations (19)):

$$\langle\cos\theta\rangle_0 = \frac{2\langle r^2(\mathrm{A},\mathrm{C})\rangle_0 - \langle r^2(\mathrm{A},\mathrm{B})\rangle_0}{2[8/(3\pi)]\langle r^2(\mathrm{A},\mathrm{C})\rangle_0} = \frac{3\pi}{8}\frac{\sigma_2}{\sigma_1} \tag{30}$$

Using *Figure 2*, we see that $\langle\cos\theta\rangle_0$ is independent of the topological distance AC = BC, being always positive and increasing with f, for $f > 2$. As examples, $\langle\cos\theta\rangle_0 = 0.28$ and 0.52 for $f = 6$ and 12, corresponding to angles of ~75° and ~60°, respectively. (The same values are obtained from equation (30) using for σ_1 and σ_2 the perturbative results in equation (19)). Otherwise said, the average angle between arms is always smaller than 90°, whereas it is equal to 90° for any f in the phantom chain. *Figure 6b* shows how the decrease of this average angle is coupled with an increase of $\langle Z^2\rangle_0$: a relatively large value of $\langle Z^2\rangle_0$ enables the macromolecule to expand over the phantom chain much less than the individual arms do. As a result of the squeezing of the average angle , the star polymer tends to assume an umbrella-like shape (see *Figure 6*).

Proceeding to consider $\langle S^2\rangle_0 = \langle X^2\rangle_0 - \langle Z^2\rangle_0$, its dependence on f is determined by the rate of change with f of $\langle X^2\rangle_0$ and $\langle Z^2\rangle_0$, so that the radius of gyration of a branched polymer may be less expanded than that of a linear chain, thus giving a minimum in the plot of α_S^2 *versus* f as in *Figure 4*. Therefore, the ratio $\alpha_S^2/\alpha_{S,\mathrm{linear}}^2$ is lower than unity at small f (= 3–4), so that g is smaller than g_{ph} (see equation (27)) for lightly branched chains, whereas the opposite is true at larger f.

For the sake of completeness, we also report in *Figure 3* the dimensionless ratio $\rho = \langle S^2\rangle_0^{1/2}/R_{\mathrm{H0}}$ as a function of f. This quantity has the advantage that it can be measured on a single sample, thus avoiding the need for a linear polymer as a reference term. Owing again to the contrasting factors discussed above in determining $\langle S^2\rangle_0$, the effect of the screened interactions is larger on R_{H0}, so that ρ is always smaller than ρ_{ph}.

The comparison of the present results with experimental data is rather difficult since most of the earlier investigations from regular stars (see, for example, refs. 1 and 2) were mainly concerned with intrinsic viscosity, which lies outside the scope of the present paper. Moreover, both the g and the h ratios were reported to be molecular-weight-dependent[5,6], so that it is not always easy to ascertain the true asymptotic values. In general, the results from relatively lightly branched stars (with f up to 6–8) are quite in agreement with our prediction as well as with those of the phantom chain. The experimental g values, averaged over different, high-molecular-weight polystyrene[1,8] and polyisoprene[2] stars, are equal to the theoretical values within experimental error. It is remarkable, however, that for $8 \gtrsim f > 3$ all the experimental points are systematically larger than g_{ph} by about 2–4%, whereas Monte Carlo simulations of star polymers on a lattice[18,19] predict still larger values. On the other hand, for $f = 3$ a few data from high-molecular-weight polystyrene stars[5] suggest g values *lower* than g_{ph}, although with some scatter, in keeping with our results and unlike Monte Carlo simulations[18,19]. The experimental results from more heavily branched polystyrene chains[4,5], having typically $f = 12$ or 18, show a larger discrepancy from theory, the g ratio being larger than both g_{ph} and our result, although close to the Monte Carlo value[19] for $f = 12$. We believe that a reason for this discrepancy lies in the strong correlation induced by the constraint of a common branch point for many arms (even though its detailed chemical structure[6,7] somehow avoids an excessive crowding at the star core). On the other hand, some ambiguity may be present in these few data, since rather large differences exist between otherwise very careful light scattering[5] and neutron scattering[6] determinations of $\langle S^2\rangle_0$, hence of g, carried out *on*

the same samples. Furthermore, the molecular-weight dependence[5,6] of the g ratio makes it difficult to extrapolate to the asymptotic value (see e.g. figure 7 of ref. 6) for a meaningful comparison with the present theoretical values.

Concerning the h ratio (see equation (25b)), the available data[4,5] are even scarcer, although being more accurate[5]: they also show some scatter and some residual molecular-weight dependence, but appear to be larger than h_{ph}. This trend is in keeping with our results, which however become quantitatively inadequate at large f because of the preaveraged hydrodynamic approximation in the Zimm limit[20] implied by equation (12). This is probably a gross oversimplification for heavily branched chains, due to the large density of segments near the star core, which excludes most of the solvent from the inner parts of the polymer. Furthermore, any hydrodynamic screening effect of the arms[21] is completely neglected; under these conditions, equation (12) is only a first approximation, so that our results may only give a qualitative trend.

THE STRUCTURE FACTOR

The structure factor $S(Q)$ was calculated numerically from equation (13) using the values of $\langle r^2(i,j)\rangle_0$ at convergence. The first-order perturbative expression is obtained upon inserting in the same equation the results given in equations (19) and carrying out the integrals over i and j:

$$S(Q)=\frac{f}{u^2}\left[\frac{2}{\sigma_1^2}\left(e^{-u\sigma_1/f}+\frac{u}{f}\sigma_1-1\right)+2\frac{f-1}{\sigma_1-2\sigma_2}\left(\frac{1}{\sigma_1}(1-e^{-u\sigma_1/f})-\frac{1}{2(\sigma_1-\sigma_2)}(1-e^{-2u(\sigma_1-\sigma_2)/f})\right)\right] \quad (31)$$

where σ_1 and σ_2 are given in equation (19c) and:

$$u=Q^2l^2N/6 \quad (31a)$$

In the limit $K/(\bar{k})^{1/2}=0$, that is, $\sigma_1\equiv 1$ and $\sigma_2\equiv 0$ (see equation (19c)), we recover the well known Benoit equation[22] for the phantom-chain star polymer.The structure factor is molecular-weight-independent when plotted as $\mu^2S(Q)$ *versus* μ^2, where $\mu^2=Q^2\langle S^2\rangle$, and is shown in this format in *Figure 7* in comparison with the Benoit equation[22]. In the latter case, we used the expression $\langle S^2\rangle_{ph}=(Nl^2/6)(3f-2)/f^2$ for consistency (see equation (20), with $\sigma_1=1$, $\sigma_2=0$) to define the variable μ (see also equation (31a)). At sufficiently small Q, developing in series equation (13), we get the familiar result:

$$1/S(Q)\simeq 1+Q^2\langle S^2\rangle/3=1+\mu^2/3 \quad (32)$$

(Obviously enough, equation (32) is also given by equation (31) for $u\to 0$, taking into account equation (20).) The usefulness of the latter equation is evident in that it is independent of the specific model chosen and of the number of arms f, unlike the peak position in the previous plot (see *Figure 7*). Our numerical results for $1/S(Q)$ *versus* μ^2 are shown in *Figure 8* in comparison with the Benoit result. Note that $S(Q)$ is bound to be smaller in the presence of the screened interactions than for the phantom-chain model, and that this effect shows up also when the structure factor is plotted as a function of $Q^2\langle S^2\rangle$, due to the non-affine expansion (e.g. see *Figure 2*).

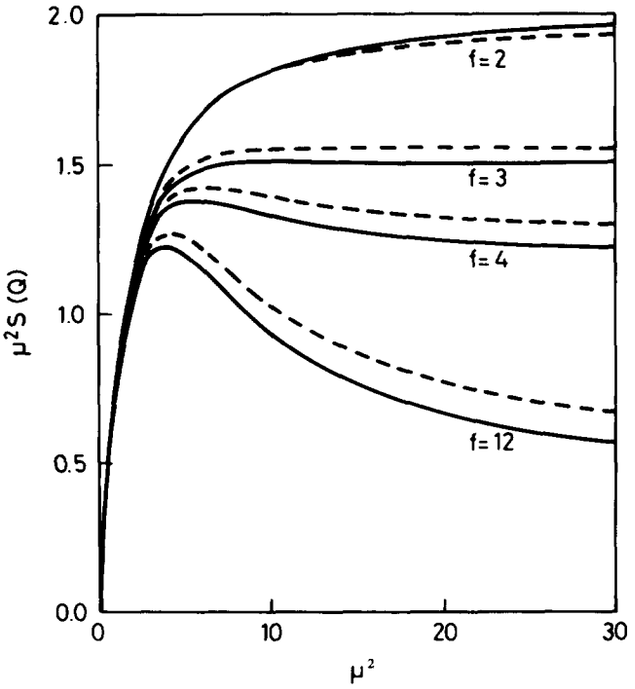

Figure 7 The structure factor $S(Q)$ plotted as $\mu^2S(Q)$ *versus* μ^2, where $\mu^2=Q^2\langle S^2\rangle$ and $Q=4\pi\sin(\theta/2)/\lambda$ is the modulus of the scattering vector. Full curves: numerical results. Broken curves: Benoit equation[22] for the phantom chain. The values of f are shown on the curves

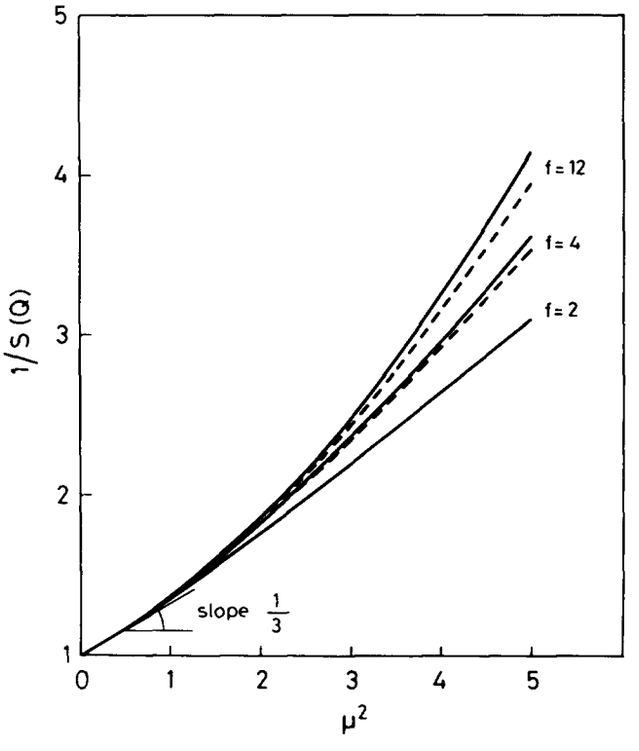

Figure 8 The reciprocal of the scattered intensity plotted as a function of $\mu^2=Q^2\langle S^2\rangle$ (see *Figure 7*). Full curves: numerical results. Broken curves: Benoit equation[22] for the phantom chain. The limiting slope of 1/3 is also shown. For the linear chain ($f=2$) the present results coincide with those of the phantom chain

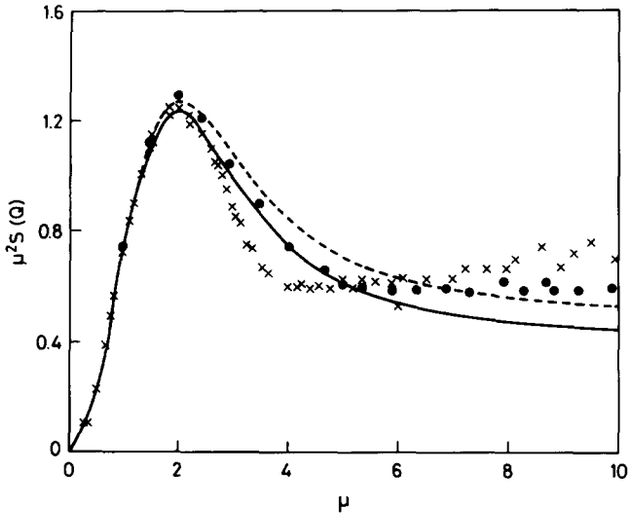

Figure 9 The experimental[7] and calculated structure factor for 12-arm polystyrene plotted as $\mu^2 S(Q)$ *versus* μ (see *Figure 7*). The molecular weights, concentrations and mean-square radii of gyration of the two samples[7] are: (×) $M_w = 55000$, $c = 2.49 \times 10^{-2}$ g cm^{-3}, $\langle S^2 \rangle_0 = 1.33 \times 10^3$ Å^2; and (●) $M_w = 467000$, $c = 2.35 \times 10^{-3}$ g cm^{-3}, $\langle S^2 \rangle_0 = 1.20 \times 10^4$ Å^2. The solvent was cyclohexane-d_{12} at $T = 35$°C (a Θ-solvent) and the results are from neutron scattering measurements (from figures 2 and 4 of ref. 7). Full curve: present numerical results. Broken curve: Benoit equation[22] for the phantom chain

From these considerations, it emerges that the peak position and height in the plot of $\mu^2 S(Q)$ *versus* μ is model-dependent, so that a fit to the Benoit equation carried out only in this region[9] is somewhat doubtful, yielding at most approximate values for the radius of gyration[7]; the situation would be even worse in a good solvent. Therefore, as suggested by Burchard[5,6], the best procedure to get $\langle S^2 \rangle$ is to use the small-angle scattering by plotting $1/S(Q)$ *versus* Q^2 and employing equation (32), even though the branched chains show an upward curvature which restricts the range of linearity (see *Figure 8*). Furthermore, this curvature is larger the higher is the degree of branching, and is enhanced by any expansion of the chain.

In *Figure 9* we report the calculated and experimental scattering curves for 12-arm regular star polystyrenes plotted as $\mu^2 S(Q)$ *versus* μ from ref. 7. The observed peak is indeed narrower than expected for the phantom chain (broken curve), in agreement with our predictions, particularly for the largest-molecular-weight sample (full circles). It should be stressed that the observed narrowing is due to the increased uniformity of the polymer density with respect to that of the phantom chain: in turn, this is related to the large fluctuations of the branch point around the centre of mass, producing the umbrella-like shape of the star polymer shown in the lower part of *Figure 6*. This experimental result is at variance with what is found for molten star polyethylenes with $3 \leqslant f \leqslant 18$, where no discrepancy was found[9] with the Benoit equation for the phantom chain[22]. This may be easily explained by considering that polyethylene is much 'thinner' than polystyrene[12], so that the screened-interactions effect would be much smaller and our result would essentially coincide with Benoit's. On the other hand,the experimental peak widths in *Figure 9* show some molecular-weight dependence, being narrower for the star polymer comprising only about 90 skeletal atoms per arm[7] (crosses), unlike our results. However, it should be pointed out that correlation between rotational states does eventually show up when short chain sequences are probed, a feature neglected for simplicity in the present work. This local stereochemical effect is responsible for the increase in scattering at larger μ (see *Figure 9*) and for the residual molecular-weight dependence of the peak width. (Correlation in rotational states, coupled with the screened-interactions effect, was effectively mimicked by Burchard through RIS (rotational isomeric states) simulations with enhanced chain stiffness[6,7] or using a worm-like chain[23] to reproduce his experimental results.) The molecular-weight dependence of the peak width would vanish with increasing arm length, so that the results from the larger-molecular-weight sample (full circles) in *Figure 9* should show the asymptotic effect of the screened interactions.

CONCLUDING REMARKS

The Θ expansion due to the screened interactions arising from the intrinsic chain thickness was considered in the present paper for regular star polymers. The corresponding medium-range potential has a longer range than the correlations among the skeletal rotations, but not long enough to alter the proportionality between the mean-square radius of gyration $\langle S^2 \rangle_0$ and the molecular weight. As a result, the chain expansion is asymptotically finite. The expansion depends on the star functionality, which determines the number of repulsive interactions between topologically close atoms. Using a realistic value for the single parameter of the screened interactions[12], the resulting g ratio, i.e. the ratio between the mean-square radius of gyration of a star polymer and that of a linear polymer with the same molecular weight (see equation (25a)), is very close to that predicted for a phantom chain. However, this agreement is somewhat fortuitous, arising from two approximations implicit in the phantom-chain model which cancel each other to a large extent: the phantom-chain model neglects the arms' expansion due to the intrinsic chain thickness, and assumes the arm directions to be uncorrelated, on average, thus underestimating the fluctuations of the branch point. These two effects are embodied respectively in the mean-square distance of the beads from the branch point, $\langle X^2 \rangle_0$, and in the mean-square distance of the latter from the centre of mass, $\langle Z^2 \rangle_0$, while $\langle S^2 \rangle_0$ is given by their difference (see equation (14)). Defining $\alpha_X^2 = \langle X^2 \rangle_0 / \langle X^2 \rangle_{ph}$ and $\alpha_Z^2 = \langle Z^2 \rangle_0 / \langle Z^2 \rangle_{ph}$, the latter ratio increases with f much more than the former one (see *Figure 5*). As a consequence, the average angle between the arm directions shrinks and the star polymer tends towards an umbrella-like shape (*Figure 6*), which becomes more pronounced with increasing f.

The agreement of the present results with the (relatively few) experimental data available is essentially satisfactory for lightly branched chains with up to 6–8 arms, but becomes poorer for more heavily branched chains, where the inter-arm correlation across the branch point becomes a relevant factor. In particular, the g ratio was found to be smaller than predicted for the phantom chain for $f = 3$, but in keeping with our result, and slightly larger for $f \geqslant 4$, the difference being within experimental error for f up to 6–8 and outside it for larger f. Some residual molecular-weight dependence might still be present in the experimental data[5,6], so that possibly the asymptotic values have not been reached yet; however, Monte Carlo simulations do indeed yield somewhat

larger g values than we get, particularly for large f[18,19]. In this context, we should also mention the theoretical results of Daoud and Cotton[24], who employed the blob model in a simple scaling approach. Since the local monomer concentration within a star changes strongly with the distance from the branch point, they assumed the blob size ξ to vary accordingly, in analogy with semidilute solutions. From the basic assumption that in any spherical shell of thickness ξ centred at the branch point one finds exactly f blobs, they got $g \propto f^{-1/2}$ for the Θ-state. This result relies essentially on the requirement of a high monomer concentration within the star, so that it should apply at most for heavily branched polymers with $f > 10$, as discussed also in ref. 19. At present, anyway, the experimental results[4,5] for $f = 12$ or 18 do not show conclusively the $f^{-1/2}$ dependence of g (ref. 19).

A stringent test of the present model is provided by the structure factor $S(Q)$, where Q is the modulus of the scattering vector. Owing to the non-affine expansion of the chain (see *Figure 2*), which may be pictorially represented by the 'umbrella-like' shape in the lower part of *Figure 6*, we predict a sharper peak in the plot of $\mu^2 S(Q)$ *versus* μ, where $\mu^2 = Q^2\langle S^2\rangle_0$, than given by the phantom-chain model. This is in good agreement with neutron scattering results from high-molecular-weight polystyrene[7], as shown in *Figure 9*.

The experimental behaviour of the branched chains was recently interpreted as evidence for residual three-body interactions in the Θ-state[19]. However, this is in contrast with the prediction that at $T = \Theta$ the residual three-body interactions should make the mean-square end-to-end distance of a linear chain *smaller* than predicted by the phantom-chain model[19,25–28]. In fact, the unperturbed state is achieved by compensating, on average, the repulsive three-body interactions by attractive two-body interactions. This requirement not only leads to a lowering of the Θ temperature[11,26,27], but also leaves an attractive unbalance at the end beads, since there are no outer beads giving rise to three-body repulsions to be compensated; hence, the contraction of the mean-square end-to-end distance if the screened interactions are ignored. This argument should basically hold also for star polymers, which have a larger share of three-body interactions than linear polymers: these interactions, beyond bringing about a further lowering of the Θ temperature[11], should make the mean-square arm length even smaller, the more so the larger f is. Actually, this was not found to be the case by Monte Carlo simulations of polymers on various lattices with an attractive potential to counter-balance the self-avoiding walk expansion[18,19,29]. The mean-square end-to-end distance of the linear chain turns out to be *larger* than expected for the phantom chain (though, of course, still proportional to the number of bonds), the expansion ratio being somewhat dependent on the lattice employed[18]. Furthermore, as shown by the Monte Carlo simulations of Bruns[29], the above proportionality is asymptotically reached from below through a term going to zero like $N^{-1/2}$, N being the number of skeletal bonds. Both these features are in keeping with the screened-interactions result[12,28] (see also equations (19) and (A.5)). Also, the increase with f of the expansion of the mean-square arm length (see *Figure 2* and equations (19) with $i = 1$, $j = N/f + 1$) is in agreement with Monte Carlo simulations[18].

In conclusion, we suggest that the residual three-body effects have only a minor influence in determining the unperturbed conformation of both linear and star polymers at their *true* Θ temperature[11], whereas a much more relevant role is played by the medium-range screened interactions accounting for the finite chain thickness[10,12,28].

ACKNOWLEDGEMENTS

This work was financially supported by the Progetto Finalizzato Chimica Fine e Secondaria, Sottoprogetto Materiali Polimerici, CNR (Italy).

REFERENCES

1 Roovers, J. E. L. and Bywater, S. *Macromolecules* 1974, **7**, 443
2 Hadjichristidis, N. and Roovers, J. E. L. *J.Polym. Sci., Polym. Phys. Edn.* 1974, **12**, 2521
3 Hadjichristidis, N., Guyot, A. and Fetters, L. J. *Macromolecules* 1978, **11**, 668
4 Roovers, J., Hadjichristidis, N. and Fetters, L. J. *Macromolecules* 1983, **16**, 214
5 Huber, K., Burchard, W. and Fetters, L. J. *Macromolecules* 1984, **17**, 541
6 Huber, K., Burchard, W., Bantle, S. and Fetters, L. J. *Polymer* 1987, **28**, 1990
7 Huber, K., Burchard, W., Bantle, S. and Fetters, L. J. *Polymer* 1987, **28**, 1997
8 Bauer, B. J., Fetters, L. J., Graessley, W. W., Hadjichristidis, N. and Quack, G. F. *Macromolecules* 1989, **22**, 2337
9 Horton, J. C., Squires, G. L., Boothroyd, A. T., Fetters, L. J., Rennie, A. R., Glinka, C. J. and Robinson, R. A. *Macromolecules* 1989, **22**, 681
10 Allegra, G. and Ganazzoli, F. *Adv. Chem. Phys.* 1989, **75**, 265
11 Ganazzoli, F. and Allegra, G. *Macromolecules* 1990, **23**, 262
12 Allegra, G. *Macromolecules* 1983, **16**, 555
13 Martin, J. E. *Macromolecules* 1984, **17**, 1263
14 Allegra, G. and Ganazzoli, F. *J. Chem. Phys.* 1985, **83**, 397
15 Zimm, B. H. and Kilb, R. W. *J. Polym. Sci.* 1959, **37**, 19
16 Zimm, B. H. and Stockmayer, W. H. *J. Chem. Phys.* 1949, **17**, 1301
17 Stockmayer, W. H. and Fixman, M. *Ann. NY Acad. Sci.* 1953, **57**, 334
18 Mazur, J. and McCrackin, F. *Macromolecules* 1977, **10**, 326
19 Batoulis, J. and Kremer, K. *Europhys. Lett.* 1988, **7**, 683
20 Zimm, B. H. *J. Chem. Phys.* 1956, **24**, 269
21 Doi, M. and Edwards, S. F. 'The Theory of Polymer Dynamics', Clarendon Press, Oxford, 1986, Sect. 5.7
22 Benoit, H. *J. Polym. Sci.* 1953, **11**, 507
23 Huber, K. and Burchard, W. *Macromolecules* 1989, **22**, 3332
24 Daoud, M.and Cotton, J. P. *J. Physique* 1982, **43**, 531
25 Stephen, M. J. *Phys. Lett. (A)* 1975, **53**, 363
26 de Gennes, P. G. 'Scaling Concepts in Polymer Physics', Cornell University Press, Ithaca, NY, 1979
27 Freed, K. F. 'Renormalization Group Theory of Macromolecules', Wiley, New York, 1987
28 Allegra, G. and Ganazzoli, F., *Macromolecules* submitted for publication
29 Bruns, W. *Macromolecules* 1989, **22**, 2829

APPENDIX

We shall briefly derive here the perturbative expressions for $\tilde{\alpha}^2(q)$ reported in equations (16). Let us start with $\tilde{\alpha}^2(q) \equiv 1$, therefore with $\langle r^2(i, j)\rangle_{ph} = l^2|i - j|$ (see equation (7)). Replacing this expression in equations (9) and taking into account equation (10), we perform the substitution $k = j - i$, since we chose $j > i$, and then carry

out the sum over the remaining index, i say. The result is:

$$\frac{1}{\tilde{\alpha}^2(q)} = 1 - \frac{5}{3}\frac{K}{m}\frac{f}{\varphi}\frac{1}{\sin^2(q/2)}\left\{2\sum_{k=\bar{k}}^{N/f}\frac{\sin^2(qk/2)}{k^{7/2}}S_1\left(k,\frac{N}{f},q\right)\right.$$
$$+(f-1)\left[\sum_{k=\bar{k}}^{N/f}\frac{\sin^2(qk/2)}{k^{7/2}}S_2\left(k,\frac{N}{f}q\right)\right.$$
$$\left.\left.+\sum_{k=N/f+1}^{2N/f}\frac{\sin^2(qk/2)}{k^{7/2}}S_3\left(k,\frac{N}{f},q\right)\right]\right\} \qquad \text{(A.1)}$$

where:

$$S_1 = (k, N/f, q) = \sum_{i=1}^{N/f+1-k}\sin^2\left[q\left(i+\frac{k-1}{2}\right)\right]$$
$$= \frac{1}{2}\left(\frac{N}{f}+1-k\right.$$
$$\left.+\frac{\sin(qk)+(-1)^{n_q}\sin[q(k-1)]}{2\sin q}\right) \qquad \text{(A.1a)}$$

$$S_2(k, N/f, q) = \sum_{i=N/f+2-k}^{N/f}\sin^2\left[q\left(i+\frac{k-1}{2}\right)\right]$$
$$= \frac{1}{2}\left(k-1-(-1)^{n_q}\frac{\sin[q(k-1)]}{\sin q}\right) \qquad \text{(A.1b)}$$

$$S_3(k, N/f, q) = \sum_{i=1}^{2N/f+1-k}\sin^2\left[q\left(i+\frac{k-1}{2}\right)\right]$$
$$= \frac{1}{2}\left(2\frac{N}{f}+1-k+\frac{\sin(qk)}{\sin q}\right) \qquad \text{(A.1c)}$$

Let us now consider the collective modes of a star polymer with $N/f \gg 1$, that is, with very long arms. Since the q values of interest are $q \ll 1$, using $\sin(q/2) \simeq q/2$, the leading term in equation (A.1) is[12]:

$$\frac{1}{\tilde{\alpha}^2(q)} \simeq \frac{1}{\tilde{\alpha}^2(0)} + \frac{5}{3}K\frac{f}{\varphi}G(q)q^{1/2} \qquad \text{(A.2)}$$

where, treating k as a continuous variable, we have put:

$$\frac{1}{\tilde{\alpha}^2(0)} = 1 - \frac{5}{3}\frac{K}{m}\frac{f}{\varphi}\left[\int_{\bar{k}}^{N/f}\frac{dk}{k^{3/2}}\left(\frac{N}{f}-\frac{1-(-1)^{n_q}}{2}k\right)\right.$$
$$\left.+(f-1)\left(\int_{\bar{k}}^{N/f}\frac{dk}{k^{1/2}}\frac{1-(-1)^{n_q}}{2}+\frac{N}{f}\int_{N/f}^{2N/f}\frac{dk}{k^{3/2}}\right)\right]$$
$$\simeq 1 - \frac{5}{3}\frac{K}{(\bar{k})^{1/2}}\frac{f}{\varphi} - \frac{5}{3}K\frac{f}{\varphi}\left(\frac{N}{f}\right)^{-1/2}S(f, n_q) \qquad \text{(A.3)}$$

and

$$S(f, n_q) = \begin{cases}(1-2^{-1/2})f - 2 + 2^{-1/2} & n_q \text{ even}\\ (2-2^{-1/2})f - 4 + 2^{-1/2} & n_q \text{ odd}\end{cases} \qquad \text{(A.3a)}$$

Furthermore, we defined:

$$G(q) = 2^{-3/2}\int_0^{qN/2f}\frac{x^2-\sin^2 x}{x^{7/2}}dx \qquad \text{(A.4)}$$

which changes slightly with the upper limit of integration $qN/2f = \pi n_q/4$ only for the smallest n_q values since the largest contribution to the integral comes from x close to 1. Therefore, neglecting the very first few modes, we may set the upper limit to infinity, thus getting a constant value for G, as done in equation (17).

Note that for the linear chain ($f = 2$), $S(2, n_q) = -2^{-1/2}$, from equation (A.3a), and $\varphi = 1$, from equation (8a), for both even and odd modes, so that:

$$\frac{1}{\tilde{\alpha}^2(0)} \simeq 1 - \frac{10}{3}\frac{K}{(\bar{k})^{1/2}} + \frac{10}{3}KN^{-1/2} \qquad \text{(A.5)}$$

NOTE ADDED IN PROOF

In *Figure 7* the continuous line reported for $f=2$ should coincide with the dashed line in the limit $N/f \to \infty$. Actually, our numerical results are slightly different because they were obtained for a discrete, finite chain. For $f > 2$ all the results are essentially exact in the same limit.